

## Characterization of the interaction between bovine pancreatic trypsin inhibitor and thiocyanate by NMR

Claude Jolivald <sup>a,\*</sup>, Anja Böckmann <sup>b</sup>, Madeleine Riès-Kautt <sup>a</sup>, Arnaud Ducruix <sup>a</sup>,  
Eric Guittet <sup>b</sup>

<sup>a</sup> *Laboratoire d'Enzymologie et de Biologie Structurales, CNRS, Bât. 34, F-91198 Gif-sur-Yvette, France*

<sup>b</sup> *Laboratoire de RMN, Institut de Chimie des Substances Naturelles, CNRS, F-91198 Gif-sur-Yvette, France*

Received 22 July 1997; revised 8 January 1998; accepted 8 January 1998

---

### Abstract

The interaction between Bovine Pancreatic Trypsin Inhibitor and thiocyanate was studied using NMR spectroscopy following several experimental approaches. The chemical shift variations of the BPTI protons in the absence and in the presence of increasing thiocyanate concentrations (up to 0.2 M) were significant ( $> 0.05$  ppm) for 30 protein protons belonging to 20 residues. The largest deviation, 0.2 ppm, was observed for the amide backbone proton of Arg42 in the absence of thiocyanate and in the presence of 40 molar equivalents of thiocyanate. The influence of the presence of thiocyanate on the electrostatic potential surrounding the protein was demonstrated by NOESY spectra selective at the water frequency: the presence of  $\text{SCN}^-$  favours acid catalysed exchange and disfavours base catalysis. However, a specific effect of thiocyanate was pointed out since the comparison of the chemical shifts in the presence of 40 molar equivalents of KSCN and KCl, respectively, showed much more as well as larger deviations compared to measurements in the absence of salt. A dissociation constant,  $K_D$ , for a 1/1 complex between BPTI and thiocyanate was calculated from chemical shifts measurements:  $K_D = 89 \pm 8$  mM. A second value,  $K_D = 99 \pm 10$  mM, was extracted from  $\text{SC}^{15}\text{N}$  relaxation time measurements. © 1998 Elsevier Science B.V. All rights reserved.

**Keywords:** Thiocyanate; BPTI; RMN; Crystallogenesis

---

### 1. Introduction

The growing of crystals suitable for X-ray diffraction has always been one of the major barriers to protein structure determination by this method. Many parameters affect the solubility and the ability of biological macromolecules to crystallize. The nature and concentration of salts are among the most influent ones. Indeed, salts are often used to purify and crystallize biological macromolecules by a salting-out process but their efficiency to affect protein solubility strongly depends on the nature of the salt. In 1888, Hofmeister [1] ranked

---

\* Corresponding author. Ecole Nationale Supérieure de Chimie de Paris, Laboratoire de Bioorganique et Biotechnologies, 11 rue P. et M. Curie, 75231 Paris cedex 05, France. Tel.: +33-01-44-27-67-54; fax: +33-01-43-26-07-70; e-mail: jolivald@ext.jussieu.fr

anions and cations according to their ability to precipitate hen egg white proteins, the major component of which is ovalbumin,  $pI = 4.6$ . The Hofmeister series, sometimes called lyotropic series, have been associated with many biological as well as chemical phenomena and extensively reviewed [2–4].

They were tested in crystallization and solubility studies on several proteins. The relative efficiency of anions to decrease the solubility of H.I. collagenase at pH 7.2 was recently evaluated [5] on the basis of the relative positions of solubility curves as a function of the ionic strength. The tested anions follow the order of Hofmeister series, except for phosphate and sulphate. A basic protein, hen egg white lysozyme [6,7], was also studied at pH 4.5. It was shown that the solubility of lysozyme is also more affected by anions than by cations. The larger effect of anions may be due to the positive net charge of lysozyme at pH values lower than the isoelectric point ( $pI = 11.1$ ). The effectiveness of anions and cations in promoting the crystallization of lysozyme followed the Hofmeister series, yet in the case of anions, the order was reversed. As a consequence, it seems that the efficiency of anions to promote crystallisation of basic proteins at  $pH < pI$  is reversed from the order given by the Hofmeister series. Leavis and Rothstein [8] studied the solubility of fibrinogen and their work led to a similar conclusion.

A better knowledge of the relationship between the macroscopic salt effects in protein solutions and their interactions at a molecular level could help interpreting the experimental results and be a basis for the prediction of solubility properties of a protein in the presence of a given added agent. Because of the long range nature of the Coulombic interactions, electrostatics play an important role in anion/protein interactions in solution, in particular via two distinct phenomena: ion binding [9,10] and modification of the electrostatic potential. Ion binding is mostly related to the biological function of the protein (ion transport or interaction between the enzyme and its substrate). It is also likely to take place out of the catalytic site, via the positively charged residues of the protein. The partial neutralisation of the charges on the protein surface leads to a decrease of the protein net charge and, consequently, of its solubility. The second effect of the influence of salt refers to their ability to modify the electrostatic potential in the vicinity of the protein, according to the Debye Hückel theory. The salt concentration determines the ionic strength of the solution and, as a consequence, the screening effect on local electrostatic interactions at the protein surface. Christoffersen et al. [11] studied the effect of KCl on the amide hydrogen exchange of bovine pancreatic trypsin inhibitor (BPTI) by NMR and showed that the NH exchange rate variations are directly correlated to calculated electrostatic potentials at the protein surface. The authors [11] concluded that the influence of the salt could therefore be reduced to its presence in the diffuse layer predicted by the double layer theory.

The proper description of the effect of salt on protein solutions must also take into account the role of water. Considering a three components system containing water, ion and protein, Arakawa and Timasheff [12] developed the concept of the preferential binding of the solvent to proteins. According to this theory, an efficient salting-out agent is excluded from the protein surroundings, resulting in an extra osmotic stress inducing protein–protein interaction and leading to precipitation. The same effect leads to the lowering of the molar partial volume of some proteins [13]. Preferential interactions are thus defined in terms of a competition equilibrium between water and the ligand for a locus on the protein surface. Such a concept underlines the tight relationship between hydration and direct binding in salt effects [14,15].

One important argument to conclude that interactions between ions and proteins can be neither strong nor specific is that precipitation or crystallization generally requires a high concentration of added salt (more than 1 M). However, it was found that rather low concentrations of thiocyanate (0.1–0.2 M) induce crystallization of lysozyme [7] and other basic proteins like erabutoxin [16], BPTI ( $pI = 10.1$ ) [17] or lysin from spermatozoa [18]. Structure determinations of erabutoxin b [19] and turkey egg-white lysozyme [20] using crystals grown in presence of thiocyanate show direct evidence for the binding of thiocyanate: in both cases, the thiocyanate ion lies close to the interface between two symmetry-related molecules (non-crystallographic for erabutoxin) and form contacts with an arginine.

The present work aims at investigating the influence of the presence of thiocyanate on BPTI solutions using NMR methods. The selection of BPTI as a model protein was motivated on one hand by the availability of the

complete NMR assignment of the protein [21] and on the other hand by the special features of BPTI solutions in presence of thiocyanate: its solubility is very low and follows the reverse order of the lyotropic series of Hofmeister. Indeed, Lafont et al. [22] showed that the effectiveness of the anions to decrease the BPTI solubility decreases following the order:  $\text{SCN}^- > \text{Cl}^- > \text{SO}_4^{2-}$ .

Given that NMR chemical shifts are highly sensitive to perturbation of proton environment, proton NMR spectra are used here to evaluate the effects of the presence of two different anions, chloride and thiocyanate. A comparison of the protein proton chemical shifts in solutions containing chloride or thiocyanate at the same concentration should therefore allow to point out a possible specific influence of  $\text{SCN}^-$ . Relaxation rate of  $\text{SC}^{15}\text{N}^-$  are measured to quantify this interaction by determining its thermodynamic equilibrium constant. Finally, we attempt to single out the role of thiocyanate on BPTI hydration and labile proton exchange rates.

## 2. Experimental

### 2.1. Sample preparation

#### 2.1.1. Chemicals

BPTI (Trasylol®) was a generous gift from Bayer (Leverkusen, Germany). Deuterium oxide (> 99%) and enriched  $\text{KSC}^{15}\text{N}$  (at.% of  $^{15}\text{N} > 95\%$ ) were purchased from Eurisotope. KSCN (analysis grade, Merck) was used as received. The water used to prepare the solutions was commercially available deionized and three-times distilled water for injectable purposes (Meram).

#### 2.1.2. Desalting of BPTI

The experimental conditions for desalting BPTI were basically those described by Riès-Kautt et al. [23] for lysozyme and detailed elsewhere [24]. X-ray fluorescence experiments have shown that desalted BPTI samples contain less than 0.2 molar equivalent of chloride. No potassium nor calcium ions could be detected by this method [24]. Desalted BPTI was dissolved in a mixture of water (0.5 ml) and deuterium oxide (60  $\mu\text{l}$ ). A 1 M KSCN solution was added to reach the desired final concentration, in the range from 1 to 40 times the protein concentration, i.e., from 1 to 40 protein molar equivalents. The pH was adjusted to 4.6 by addition of HCl 0.1 M (the amount of added chloride anions corresponds to 6 protein molar equivalents). The final BPTI concentration was around 5.5 mM, as measured spectrophotometrically at 280 nm using an extinction coefficient  $E^{1\text{ cm}} = 5.08 \times 10^3 \text{ M}^{-1} \text{ cm}^{-1}$ .

### 2.2. NMR measurements

#### 2.2.1. $^1\text{H}$ NMR measurements

Two-dimensional HOHAHA [25] and nuclear Overhauser effect spectroscopy (NOESY) [26] spectra were recorded for each sample on a Bruker AM400 instrument at 291 K. The mixing times were 80 ms and 200 ms for the HOHAHA and the NOESY experiments, respectively. Each two-dimensional spectrum was collected with 2 K data points in  $t_2$  and 512 data points in  $t_1$ . The sweep width was 4807 Hz. For each  $t_1$  value, 64 scans were averaged, except for the sample containing 40 molar equivalents, for which only 32 scans were averaged. Presaturation was used for  $\text{H}_2\text{O}$  suppression during the 1 s relaxation delay. The data were transferred to a IBM 6000 Risc workstation and processed using the GIFA (version 2.5) software [27]. Prior to Fourier transform, the data sets were multiplied by a pure cosine function in the  $t_1$  dimension and a square sine function shifted by  $\pi/6$  in the  $t_2$  dimension and then zero-filled to 1 K data points in  $t_1$ . The final resolution along  $t_2$  is approximately 5 Hz (0.012 ppm). Chemical shifts are measured with respect to the chemical shift of HDO set at 4.8 ppm.

### 2.2.2. NOESY spectra selective at the water frequency

One-dimensional NOESY spectra selective at the water frequency were taken using the selective excitation scheme developed by Böckmann and Guittet [28]. The mixing time was set at 100 ms and 120 ms for the spectra of BPTI in the absence and in the presence of  $\text{SCN}^-$ , to account for the efficiency of the radiation damping under these conditions. The samples of BPTI alone and of BPTI in the presence of 40 equivalent  $\text{SCN}^-$  described above were used. Spectra were acquired at a temperature of 291 K using a Bruker 600 MHz spectrometer equipped with an autoshielded gradient unit. Data were multiplied by cosine functions prior to Fourier transform. The residual water signal was suppressed using linear prediction of the GIFA program [27]. The interscan delay was 6 s and the total recording time was 50 min.

### 2.2.3. $\text{SC}^{15}\text{N}$ longitudinal relaxation time ( $T_1$ ) measurements

The NMR samples containing  $^{15}\text{N}$  enriched thiocyanate were prepared as described in the previous section and were transferred to the NMR tubes. The tube content was then degassed with a dry nitrogen flush for at least 15 min before the tubes were capped.  $^{15}\text{N}$  NMR measurements were made on a AM400 Bruker spectrometer operating at 40.554 MHz with  $\text{D}_2\text{O}$  for frequency lock. The FIDs were collected as 2 K data points and the sweep width was adjusted to give a 0.25 Hz resolution.

The  $T_1$  values for the  $^{15}\text{N}$  labelled thiocyanate solution were measured by an inversion recovery sequence (180- $\Delta$ -90-AQ). Typically, 10  $\Delta$  values were used ranging from 0.01 s to 150 s with a regular spacing in intensity. For each  $\Delta$  value, 16 scans were averaged, with relaxation delays of at least five estimated  $T_1$  ( $5 \times 50$  s). The  $T_1$  values were extracted by a nonlinear least-square fitting routine provided by Bruker.

## 3. Results

### 3.1. Resonance assignments of the 2D $^1\text{H}$ NMR spectra

Chemical shifts were measured on the HOHAHA spectra. NOESY spectra were used to lift ambiguities due to some chemical shift degeneracies. Resonance assignments of BPTI at 291 K were obtained starting from the previously published assignments at 309 K [21]. Thanks to this information, the chemical shifts of most BPTI protons have been determined. However, no crosspeaks could be assigned to any protons of the Arg1 and Pro13 residues. Several side-chain protons are also missing:  $\text{CH}_\alpha$  of Asn44, Gln31, Phe33 and Tyr35,  $\text{CH}_\beta$  of Arg20, Ile29 and Arg53,  $\text{CH}_\gamma$  of Ile18 and Ile19 and  $\text{CH}_\epsilon$  of Met52. The explanation for some of these missing crosspeaks was the overlap of the  $\text{H}_\alpha$  protons with the  $\text{H}_2\text{O}$  signal. Increasing the temperature from 291 to 309 K allows to recover the signal measured by Wagner at the same temperature. The NH proton of Gly37 is missing in Wagner's data and was assigned at 8.83 ppm. Three additional protons of the side-chain of Lys15 could also be identified at 291 K. The most significant gap between the two data sets is observed for one of the  $\text{CH}_\alpha$  proton of Cys28 at 3.63 ppm instead of 3.91 ppm in the work of Wagner. It can be noticed that chemical shift variations larger than 0.1 ppm were found between the two data sets for one third of the NH protons and that in all cases, the signal shifted to lower field at 291 K as compared to 309 K due to a smaller thermal motion.

### 3.2. Chemical shift variations of BPTI protons in the presence of thiocyanate

We measured the chemical shift variations of BPTI protons as a function of the concentration of thiocyanate. Four thiocyanate concentrations were used: 1, 10, 25 and 40 molar equivalents (0.05 to 0.2 M). For each thiocyanate concentration, the chemical shift of every proton, whose crosspeak had been assigned, was compared to its value in a solution of BPTI at the same concentration in the absence of thiocyanate.

Table 1

Most significant BPTI proton chemical shift variations, ( $\Delta\delta = \delta_{\text{BPTI} + \text{anion}} - \delta_{\text{BPTI}}$ ), in the presence and in the absence of 40 molar equivalents thiocyanate

	$\Delta\delta$ Backbone NH	$\Delta\delta$ Side-chain H $0.05 < \Delta\delta < 0.07$
<i>Charged residues</i>		
Arg17	−0.06	—
Arg39	−0.07	$\delta\text{H}$
Arg42	−0.20	$\delta\text{H}$ , $\varepsilon\text{H}$
Arg53	—	2 $\gamma\text{H}$
Lys15	−0.09	$\gamma\text{H}$ , $\delta\text{H}$
Lys26	—	$\gamma\text{H}$ , $\varepsilon\text{H}$
Lys46	−0.06	$\gamma\text{H}$
Glu7	—	$\gamma\text{H}$ , $\beta\text{H}$
Glu49	−0.05	$\gamma\text{H}$
Asp50	—	$\beta\text{H}$
<i>Neutral residues</i>		
Phe4	−0.08	—
Leu6	—	$\beta\text{H}$
Pro8	—	$\delta\text{H}$
Cys14	—	$\beta\text{H}$
Ala16	+0.06	—
Ile18	—	$\delta\text{H}$
Ile19	−0.05	—
Cys30	−0.10	—
Val34	−0.05	—
Cys38	—	$\beta\text{H}$
Thr32	−0.04	—
Ala48	−0.04	—

BPTI 5.5 mM, pH 4.6,  $T = 18^\circ\text{C}$ .

Among the protons whose chemical shift remained unchanged, one can find most of the buried aromatic residues of BPTI: Tyr10, Tyr21, Tyr23, Phe22 and Phe45. This result precludes the possibility of any systematic error in chemical shift evaluation. A significant (i.e., larger than 0.05 ppm) change in the chemical shift was observed for 30 protons, which are located on one third of a total of 58 residues. Eleven backbone amide protons and 19 side-chain protons are concerned. The variation range of the chemical shifts for all protons remains less than 0.2 ppm and is maximum for 40 molar equivalents of thiocyanate (Table 1). No significant, i.e., superior to the resolution, chemical shift variation was observed between a solution of BPTI without thiocyanate and a solution containing 1 molar equivalent thiocyanate. When increasing the concentration of thiocyanate, the deviation became higher than the resolution. Four backbone amide protons are involved in chemical shift variations larger than 0.07 ppm: Arg42, Cys30, Lys15 and Phe4. For seven other residues, the variation remained between 0.05 and 0.07 ppm. Two striking features characterize these chemical shift changes. First, except for the NH group of Ala16, the chemical shift decreased when the concentration of thiocyanate increased. Second, the backbone amide protons are more affected than side-chain protons, as illustrated in Fig. 1 for Arg42.

However, significant chemical shift changes ( $> 0.05$  ppm) were observed for 18 side-chain resonances. All charged residues, whose assignment has been at least partly achieved, were concerned, except Asp3 and Arg20. Five protons belonging to neutral side-chains also showed significant changes, among them, the  $\text{C}_\beta\text{H}$  protons of Cys14 and Cys38. All side-chain proton resonances moved upfield, as shown for Glu7 in Fig. 2.

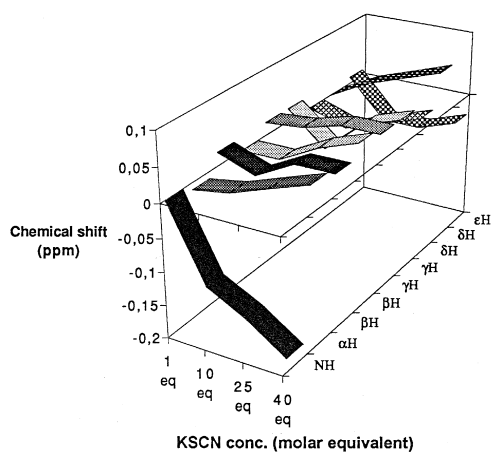


Fig. 1. Three-dimensional plot of the variation of the chemical shift of the protons of Arg42 as a function of the thiocyanate concentration. The BPTI concentration is 5.5 mM.  $T = 18^{\circ}\text{C}$  and  $\text{pH} = 4.6$ .

### 3.3. Chemical shift variations in the presence of KCl

Chemical shift variations of BPTI protons were measured between a 5.5 mM BPTI solution containing 0 and 40 molar equivalents KCl, in addition to the six equivalents used for pH adjustment, also present in the thiocyanate solutions. Only two protons exhibited chemical shift variations higher than 0.04 ppm. The chemical shift of one of the  $H_{\gamma}$  protons of the side-chain of Lys15 increased by 0.05 ppm after adding 40 molar equivalents KCl to the BPTI solution. The second change had a greater amplitude: 0.07 ppm chemical shift variation was measured for the backbone amide proton of Arg42.

### 3.4. Study of the hydration and the exchange rates of labile protons

In order to study the influence of thiocyanate on the hydration and on the rates of labile protons exchange of BPTI, one- and two-dimensional spectra selective at the water frequency [29,28] were recorded. In these spectra,

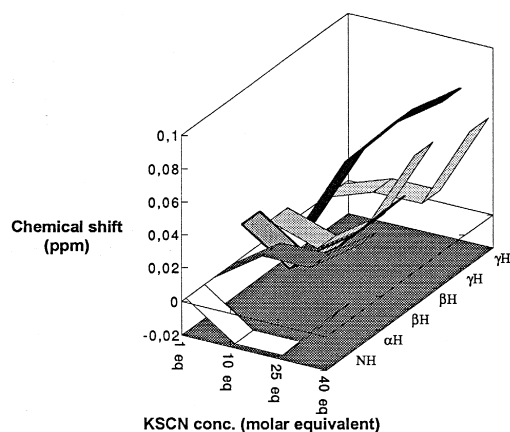


Fig. 2. Three-dimensional plot of the variation of the chemical shift of the protons of Glu7 as a function of the thiocyanate concentration. The BPTI concentration is 5.5 mM.  $T = 18^{\circ}\text{C}$  and  $\text{pH} = 4.6$ .

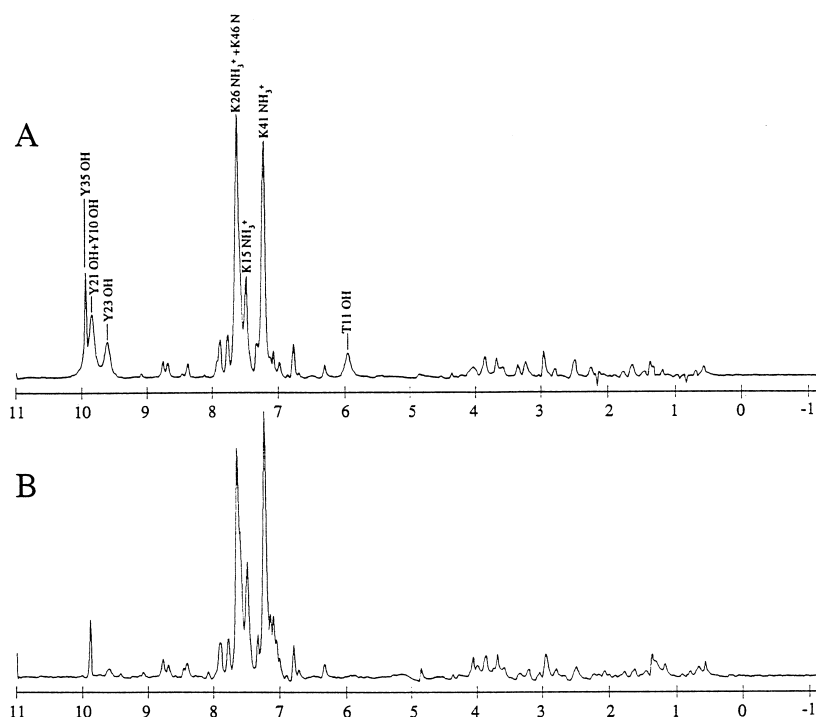


Fig. 3. Water selective NOESY spectra recorded at 293 K using the samples described in the text in the absence of thiocyanate (A) and in the presence of 40 equivalents thiocyanate (B). Resolved resonances are assigned. Experimental parameters are described in Section 2.

only the resonances taking their origin at the water frequency are observable, they step from NOE interactions between protein protons and internal water molecules and exchange of labile protons with water. Fig. 3 shows the NOESY spectra selective at the water frequency for BPTI alone (Fig. 3A) and in the presence of 40 equivalent thiocyanate ( $\text{SCN}^-$ ) (Fig. 3B).

The most striking difference between the two spectra is the variation of the intensities of the hydroxyl proton exchange peaks. The resonances of Tyr10, Thr11, Tyr21 and Tyr23 hydroxyl protons are much broadened or no longer observed upon addition of salt; in contrast, Tyr35 still shows a narrow exchange peak, but of weaker intensity. This indicates that exchange of this proton is somewhat slowed down. On the other hand, the broadened resonances of the first four hydroxyl protons indicate accelerated exchange (in contrast to our preliminary interpretation [28]). These four protons have been shown to exchange by acid catalysis at pH 4.5 [30]. The hydroxyl proton of Tyr35 is the only one exchanging by base catalysis at this pH, this is due to the restricted access to its hydroxyl oxygen which makes acid catalysis unfavourable [30].

The salt effects are also observable in 2D NOESY–TOCSY spectra selective at the water frequency taken in absence and in presence of 40 equivalent  $\text{SCN}^-$  [28]. Several observations could be made and can be summarised as follows. The crosspeaks between hydroxyl protons of Thr11 and Tyr23 and nearby ( $d < 3 \text{ \AA}$ ) aliphatic protons are getting more intense in the presence of  $\text{SCN}^-$ , as expected for accelerated exchange. The intensity of the crosspeak between the hydroxyl proton of Tyr35 and its  $\beta$ -proton is not much altered by the presence of the salt. Crosspeaks with the hydroxyl protons of Tyr10 and Tyr21 are not observed.

As no external reference was used to calibrate the peak intensities, only relative changes in crosspeak intensities can be reported. Compared to the crosspeaks with the hydroxyl protons of Thr11 and Tyr23, crosspeaks between protein protons and protons of internal water molecules do not show the same increase in intensity. Most show a behaviour similar to that of the crosspeak between Tyr35 and its  $\beta$ -proton; the weakest

crosspeaks disappear upon addition of salt. The  $\text{NH}_3^+$  protons of lysines 26, 46, 15 and 41 give by far the strongest crosspeaks in the spectra. Their exchange rates seem not to be influenced by the presence of thiocyanate as indicated by the nearly unaltered intensities of the observed cross signals. In the 2D spectra, the crosspeaks of the  $\text{CH}_{\delta 2}$  and  $\text{CH}_{\epsilon 2}$  protons of Lys15, Lys26 and Lys46 change from negative in the absence of  $\text{SCN}^-$  to positive in the presence of 40 equivalent  $\text{SCN}^-$ . Two different phenomena can contribute to the origin of these crosspeaks: direct NOE with water giving rise to positive or negative NOEs crosspeaks, depending on the residence time of the water molecules, or chemically relayed NOE by interactions with the labile  $\text{NH}_3^+$  protons giving rise to positive crosspeaks [31]. The observed signal is the sum of the two contributions. As the exchange behaviour of the  $\text{NH}_3^+$  protons appears not to be changed, we assume that the contribution from chemically relayed NOE is still the same, while the amount of direct NOE is reduced. The change in sign of the crosspeaks thus seems to indicate reduced residence times of surface water molecules near the lysine side-chains of Lys15, Lys26 and Lys46. Other possible interpretations of the changes in sign are variations of intramolecular motions [32] or of geometrical factors governing the water proton/protein proton intermolecular relaxation [33].

### 3.5. Determination of a thermodynamic equilibrium constant

#### 3.5.1. From $^1\text{H}$ NMR data analysis

In an attempt to quantitatively address the problem, we considered that the interaction between BPTI and thiocyanate responsible for the Arg42 NH chemical shift variation can be described as a binding of the anion to the protein according to the following equilibrium:



with

$$K_D = \frac{[\text{BPTI}][\text{SCN}^-]}{[\text{BPTI}(\text{SCN}^-)]} \quad (2)$$

$K_D$  is the dissociation equilibrium constant. The NH Arg42 chemical shift variations were analyzed according to a two-site model which assumes that the experimental chemical shift is the sum of two chemical shifts, one for the Arg42 NH when it interacts with  $\text{SCN}^-$ ,  $\delta_{\text{bound}}$ , and a second for the Arg42 NH when it is free in solution,  $\delta_{\text{free}}$ . This model is described by the following relationship:

$$\delta_{\text{obs}} = x_{\text{bound}} \delta_{\text{bound}} + x_{\text{free}} \delta_{\text{free}} \quad (3)$$

where  $\delta_{\text{obs}}$  is the observed chemical shift at a given concentration of  $\text{SCN}^-$ . Where  $x_{\text{bound}}$  and  $x_{\text{free}}$  are the molar fractions of the bound and free BPTI, respectively.  $\delta_{\text{free}}$  is determined experimentally. Taking material balances into account, molar fractions can be expressed as a function of  $K_D$  and  $E_0$  and  $S_0$ , the total concentrations of BPTI and thiocyanate in solution, respectively. Finally,  $\delta_{\text{obs}}$  can be expressed as:

$$\delta_{\text{obs}} = \delta_{\text{free}} + \frac{(\delta_{\text{bound}} - \delta_{\text{free}}) \times \left\{ (S_0 + E_0 + K_D) - \sqrt{(S_0 - E_0 + K_D)^2 + 4K_D E_0} \right\}}{2E_0} \quad (4)$$

A four experimental data set was fitted to this equation to determine  $K_D$  and  $\delta_{\text{bound}}$ . Fig. 4 shows a plot of the variation of the chemical shift of the amide proton of Arg42 as a function of  $\text{SCN}^-$  concentration. The solid line is the best theoretical fit of the data to Eq. (4), giving  $K_D = 89 \pm 8$  mM and  $\delta_{\text{bound}} = 8.12 \pm 0.1$  ppm.



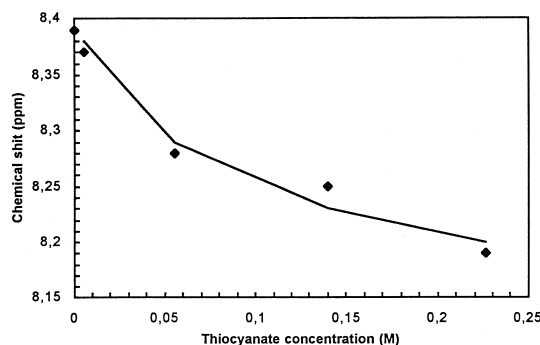


Fig. 4. Comparison of experimental (symbols) and simulated data (solid line) for the chemical shift variation of NH Arg42 as a function of KSCN concentration.  $T = 18^\circ\text{C}$ ,  $\text{pH} = 4.6$ .

### 3.5.2. From $\text{SC}^{15}\text{N}^-$ relaxation times ( $T_1$ ) analysis

Since relaxation parameters correlate with structural features of molecules, and particularly with their motions, relaxation rate measurements are likely to provide relevant information on changes in the environment of thiocyanate in the presence of BPTI. The  $^{15}\text{N}$  relaxation time of 0.22 M thiocyanate,  $\text{pH} 4.5$  was found to be rather large: around 74 s, which is consistent with the 80 s relaxation time reported by Crull and Goff (1993) [36] in a 0.1 M thiocyanate,  $\text{pH} 6.8$ . In the present work, 0.22 M  $\text{SC}^{15}\text{N}$  solutions were titrated with various amounts of BPTI (0.01 to 4.3 mM) at  $\text{pH} 4.5$ . Fig. 5 shows that the relaxation time of thiocyanate strongly decreased at increasing concentrations of BPTI, down to 10 s at a 4.3 mM BPTI concentration. Assuming a two-state model, the observed relaxation rate can be expressed as:

$$R_{\text{obs}} = x_{\text{bound}} \cdot R_{\text{bound}} + x_{\text{free}} R_{\text{free}} \quad (5)$$

with  $R = 1/T_1$  being the  $^{15}\text{N}$  relaxation rate.

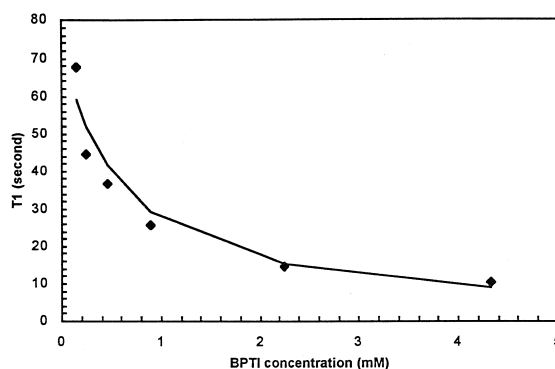


Fig. 5. Relaxation times of  $\text{SC}^{15}\text{N}$  at  $18^\circ\text{C}$  and  $\text{pH} 4.6$  as a function of BPTI concentration. The concentration of KSCN was 0.22 M. The solid line represents the nonlinear least square best fit of the data. The relaxation time of 0.22 M  $\text{SC}^{15}\text{N}$  at  $18^\circ\text{C}$  and  $\text{pH} 4.6$  in the absence of BPTI is at 74 s.

Again, the complexation process described by Eq. (1) is assumed to occur. From mass balances and Eqs. (2) and (5),  $R_{\text{obs}}$  can be expressed as a function of  $E_0$ ,  $S_0$ , respectively, the total concentrations of BPTI and thiocyanate and two parameters  $K_D$ ,  $R_{\text{bound}}$ :

$$R_{\text{obs}} = R_{\text{free}} + \frac{(R_{\text{bound}} - R_{\text{free}}) \times \left\{ (S_0 + E_0 + K_D) - \sqrt{(E_0 - S_0 + K_D)^2 + 4K_D E_0} \right\}}{2S_0} \quad (6)$$

The two parameters were adjusted from Eq. (6) by minimization of the difference between calculated and experimental  $R_{\text{obs}}$  values. The best fit was obtained with  $K_D = 99$  mM and  $T_{1 \text{ bound}} = 0.136$  s with a relative standard deviation of 10.6%.

#### 4. Discussion

Measurements of chemical shift variations of BPTI protons in the absence and in the presence of increasing thiocyanate concentrations (up to 0.2 M) showed that the chemical shifts of 30 protons belonging to more than one third of the residues were affected by the presence of the salt. However, the chemical shift variations measured in presence of 40 molar thiocyanate equivalents remain rather weak: the largest deviation is 0.2 ppm for the amide backbone proton of Arg42. The second most important one is less than one half: 0.09 ppm for the amide backbone proton of Lys46. Most of the significant chemical shifts changes ( $> 0.05$  ppm) are less than 0.07 ppm. These results, in addition to the fact that no significant modification of the NOESY maps in terms of crosspeak intensities, demonstrate that the solution structure of BPTI is not significantly affected by the presence of  $\text{SCN}^-$ . The same observation was reported by Christoffersen et al. [11] in a study on the effect of KCl on the hydrogen exchange in BPTI.

##### 4.1. Evaluation of the effects of the variation of the electrostatic potential

In a recent publication, Christoffersen et al. [11] studied the influence of increasing KCl concentration on BPTI, which is a system very close to ours. He pointed out a very good correlation between the salt effect on proton exchange (measured as the slope of the variation of some BPTI amide protons exchange rate against the salt concentration) and the local electrostatic potential at the surface (calculated from the Poisson–Boltzman equation and using crystallographic coordinates). The correlation was also verified for buried amide protons, leading again to the conclusion that the mechanism of hydrogen exchange does not require any deviation from the crystal structure and, as a consequence, that salt concentration variations do not induce any conformational modification of the protein. This result appears not to be verified for all proteins (for example,  $\alpha$ -chymotrypsin was shown to be a salt-dependent equilibrium mixture of active and inactive conformers in solution [34]), but is verified here with  $\text{SCN}^-$  replacing  $\text{Cl}^-$ . In addition, the present study seems also to corroborate their observation on the proton exchange but seen from the fast exchanging protons. Namely, NOESY spectra selective at the water frequency show that the same salt effects are observed in the presence of KCl or KSCN: acid-catalysed exchange of hydroxyl protons is favoured in the presence of salt and base catalysed exchange is slowed down. The observed phenomenon can be explained by the salt-dependent polarization of the solution surrounding the protein; an increase in the ionic force in the presence of  $\text{SCN}^-$  favours acid-catalysed exchange and unfavours base catalysis. The effect observed upon addition of  $\text{SCN}^-$  is comparable to the one observed when lowering the pH [30]. The BPTI spectrum in the presence of 40 equivalent  $\text{SCN}^-$  at pH 4.5 is very similar to the spectrum of BPTI observed at pH 3.2.

Chemical shifts are sensitive to the electric field, and could be good reporters for its variations. To test whether the observed chemical shift variations were only due to a screening effect, the BPTI protons chemical shift variations in absence and in presence of 40 molar KCl and 40 molar KSCN equivalents were compared.

Only two significant ( $> 0.05$  ppm) changes were observed with 40 molar KCl equivalents: the lowering of the chemical shift of the amide proton of Arg42, 0.07 ppm, and of  $\text{CH}_\gamma$  of Lys15, 0.05 ppm. These protons were also found to be affected in the presence of 40 molar KSCN equivalents but results differ much in terms of amplitude of the variations: chemical shift variations are three times larger for NH Arg42 in a KSCN solution and twice higher for  $\text{CH}_\gamma$  of Lys15. Chemical shift variations can thus be ascribed to two additive effects. The first contribution arises from the screening effect on the electrostatic field at the BPTI surface while the second one could account for a more specific effect of the anion used to change the ionic strength, the later effect being more important for  $\text{SCN}^-$  than for  $\text{Cl}^-$ . This could be interpreted in terms of a greater selectivity of  $\text{SCN}^-$  for BPTI.

#### 4.2. Evidences for $\text{SCN}^-$ / BPTI interactions. Evaluation of an affinity constant

To test further this hypothesis, we performed relaxation measurements and chemical shift variation analyses to unravel possible interactions. A  $\text{SCN}^-$ /BPTI binding constant was extracted from the computer fit of the chemical shift of Arg42 NH as a function of the total thiocyanate and protein concentrations [35].  $\text{SC}^{15}\text{N}^-$  relaxation time measurements were alternatively used to extract the same parameter [35,36]. The two parallel methods yield  $K_D$  values of respectively  $89 \pm 8$  mM and  $99 \pm 9$  mM for the binding of  $\text{SCN}^-$  to BPTI at pH 4.5, assuming a 1:1 binding ratio. The extent of agreement between the theoretical and the experimental results in both cases as well as the very similar results calculated from experimental results using two different approaches (fit of chemical shifts variation and relaxation time analysis) suggests that the model used in the calculations reproduces the essential features of the interaction. The value of the dissociation constant is high, indicating a low affinity of thiocyanate to BPTI, which contrasts with the ability of this anion to decrease the solubility of the protein [22]. Rather high values of dissociation constant are also reported in the literature, even for proteins whose biological function is to interact with inorganic anions. As an example, AE1 is a protein responsible for the tightly coupled exchange of chloride for bicarbonate in the respiratory cycle of the organism. Chloride and bicarbonate are thus two physiologic substrate for AE1. The dissociation constants determined from line broadening measurement were  $K_D = 6.9 \pm 0.9$  mM and  $74 \pm 10$  mM for, respectively, nitrate, which is a structural analog of bicarbonate, and chloride [37]. Even more relevant examples—as far as thiocyanate is concerned—deal with the interaction of thiocyanate with peroxidases, proteins known to catalyse oxidation of inorganic ions, including  $\text{SCN}^-$ . Chemical shift changes of the proton resonances of the methyl groups 1 and 8 of the heme group of horseradish peroxidase in the presence of various amounts of thiocyanate yielded  $K_D$  values of 166 and 136 mM, respectively [35]. It has also been shown that  $\text{SCN}^-$  interacts with lactoperoxidase, in the heme pocket of the enzyme, with a  $K_D = 90 \pm 5$  mM [38] or  $113 \pm 10$  mM [36] from  $^{15}\text{N}$  relaxation measurements. The value of the dissociation constant between thiocyanate and BPTI determined in the present work are thus strikingly similar to those determined independently by Crull and Goff [36] and Modi et al. [38] for the thiocyanate/lactoperoxidase complex.

#### 4.3. Is a direct interaction between BPTI and thiocyanate plausible?

Many of the BPTI protons for which chemical shifts were found to significantly vary in presence of KSCN belong to the side-chain of basic residues. Thus,  $\text{SCN}^-$ /BPTI interactions are likely to occur by an electrostatic interaction leading to a partial charge neutralization. However, about one fourth of the backbone amide protons as well as five neutral side-chain protons are also affected by the presence of thiocyanate and this sole interaction cannot account for all the observed effects. Thiocyanate possibly interacts with some protein hydrogen donors such as main chain amide protons [39].

The localization of the protons involved in chemical shift changes in the three-dimensional structure of the protein is also of interest. Three different domains at the protein surface are concerned. A first set comprises residues 14 to 19 and residue 38 near the active site. This could be associated with a conformational flip of the

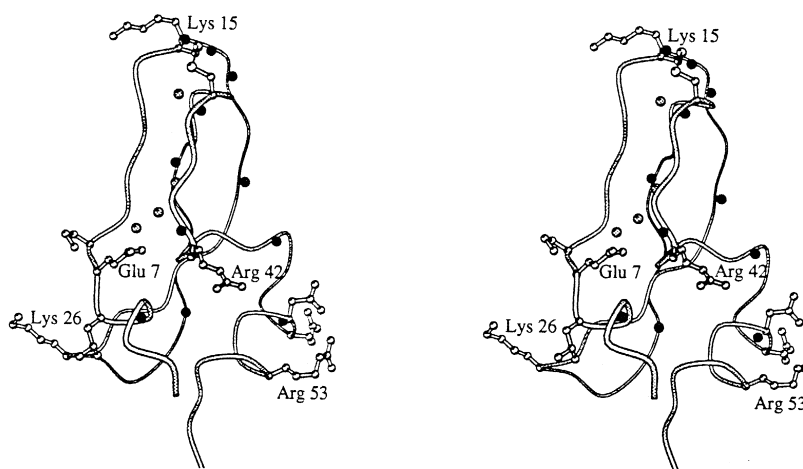


Fig. 6. Localization of the internal water molecules in BPTI spatially correlated to some of the residues having important chemical shift variations on the three-dimensional structure of BPTI. Crystallographic data 4PTI.

Cys14–Cys38 disulphide bridge which has been observed in previous NMR measurements [40]. The second group, including Phe4, Arg42 and Glu7, lies at one end of the antiparallel  $\beta$ -sheet, near the loop formed by residues 25 to 28. Finally, the third one includes three residues belonging to the C-terminal  $\alpha$ -helix: Lys46, Glu49 and Asp50. According to Chakrabarti [39] who analyzed sulphate and phosphate binding sites in 34 proteins, such structural patterns (namely peptide NH groups or peptides at the *N*-terminus of helix, as well as near  $\beta$ -turns) are likely to be suitable environments for anion binding. However, it must be noticed that, in case of BPTI the localisation of the two phosphate ions are somewhat different: one lies at the side-chain extremity of Arg20 whereas the second one is close to the hydroxyl group of Tyr35.

Fig. 6 shows that the chemical shift changes implicate residues close to the four internal water molecules of BPTI. These internal water molecules have been described in the BPTI crystallographic structure [41] and were also observed by NMR [42]. One lies in a pocket near the 14–38 disulphide bridge. The others are located in a cleft between residues 8 to 10 and residues 40 to 44. The bottom of the cleft is occupied by the aromatic ring of Phe33. This cavity containing the internal water molecules is open to the solvent when the side-chain of Glu7 is in one of its alternate conformations [43]. This site is thus exposed to solvent property changes while being quite structured since two of the inner water molecules are tetrahedrally coordinated. Since ion binding to protein has been very often correlated to hydration phenomena [44], we attempted to get an insight on the influence of thiocyanate on BPTI hydration state by studying the residence time of water molecules in the protein vicinity. However, 2D NOESY–TOCSY spectra selective at the water frequency in the presence or absence of 40 equivalents thiocyanate do not allow to observe significant changes in the crosspeaks between protein protons and the protons of internal water molecules. These observations seem to indicate that no or only a weak influence of thiocyanate on the residence times of internal water molecules. Unfortunately, at present, there is no method available allowing an accurate estimation of the influence of external parameters on residence times of internal water molecules [45,46] that could confirm that observation.

## 5. Conclusions

The present NMR study of the influence of  $\text{SCN}^-$  on BPTI in solution leads to the following conclusions.

(1) The influence of salts can be described in terms of two different contributions: modification of the electrostatic potential at the protein surface and local interactions with BPTI.

(2) The modification of the electrostatic potential at the protein surface is confirmed by the observed exchange rate variations of hydroxyl protons of BPTI. The correlation between the type of catalysis and the changes in exchange rates observed for the hydroxyl protons in the presence of  $\text{SCN}^-$  correspond to those observed for slow exchange rates of amide protons in the presence of  $\text{Cl}^-$  [11]. To evaluate possible inherent effects of  $\text{SCN}^-$ , it would be interesting to compare the effects of  $\text{SCN}^-$  on the exchange rates of the hydroxyl protons to those induced by other salts to assess whether or not the observed effects originate exclusively from changes in the electrostatic potentials, and to analyze the effect of thiocyanate on the exchange rate of the slowly exchanging amide protons.

(3) A specific effect of thiocyanate was observed from chemical shift measurements and relaxation measurements. The dissociation constant for the interaction of  $\text{SCN}^-$  with BPTI, as measured at pH 4.5 by two parallel methods (fit of chemical shifts variation and relaxation time analysis) is rather high ( $89 \pm 8$  mM and  $99 \pm 9$  mM, respectively), indicating a low affinity of thiocyanate to BPTI.

(4) The corresponding interaction sites are not limited to the basic side-chains but also implies several sites on the protein surface.

The results can be interpreted according to the binding theory developed for colloid solutions and then applied to protein solutions [47]. The binding can be explained by a simple two-state model in which ions bind in two different loci, one locus being the surface itself, which may or may not contain different binding sites, the second locus being the diffuse part of the double layer. Depending on the system, binding in one locus is preferred over binding in the other.

## Acknowledgements

We thank Bayer (Leverkusen, Germany) for a generous gift of BPTI (Trasylol®).

## References

- [1] F. Hofmeister, Arch. Exp. Pathol. Pharmacol. 24 (1888) 247.
- [2] P.H. von Hippel, T. Schleich, in: S.N. Timasheff, G.D. Fasman (Eds.), Structure and Stability of Biological Macromolecules, Dekker, New York, 1969, p. 417.
- [3] K.D. Collins, M.W. Washabaugh, Q. Rev. Biophys. 18 (1985) 323.
- [4] K.D. Collins, Biophys. J. 72 (1997) 65.
- [5] C. Caronnaux, M. Riès-Kautt, A. Ducruix, Protein Sci. 4 (1995) 2123.
- [6] J.P. Guilloteau, M. Riès-Kautt, A. Ducruix, J. Cryst. Growth 122 (1992) 223.
- [7] M. Riès-Kautt, A. Ducruix, J. Biol. Chem. 264 (2) (1989) 745.
- [8] P. Leavis, F. Rothstein, Arch. Biochem. Biophys. 161 (1974) 671.
- [9] M.T. Record Jr., C.F. Anderson, T.M. Lohman, Q. Rev. Biophys. 11 (2) (1978) 103.
- [10] S. Linse, B. Jönsson, W.J. Chezin, Proc. Natl. Acad. Sci. U.S.A. 92 (1995) 4748.
- [11] M. Christoffersen, S. Bolvig, E. Töchsen, Biochemistry 35 (1996) 2309.
- [12] T. Arakawa, S.N. Timasheff, Methods Enzymol. 114 (1985) 49.
- [13] P.E. Pjura, M.E. Paulaitis, A.M. Lenhoff, AIChE J. 41 (4) (1995) 1005.
- [14] K.D. Collins, Proc. Natl. Acad. Sci. U.S.A. 92 (1995) 5553.
- [15] V.A. Persegian, Nature 378 (1995) 335.
- [16] M. Riès-Kautt, A. Ducruix, J. Cryst. Growth 110 (1991) 20.
- [17] A. Ducruix, M. Riès-Kautt, in Methods: A Companion to Methods in Enzymology, Vol. 1, 1990, p. 25.
- [18] T.C. Diller, A. Shaw, E.A. Stura, V.D. Vacquier, C.D. Stout, Acta Cryst. D 50 (1994) 620.
- [19] P. Saludjian, T. Prange, J. Navaza, J.P. Guilloteau, M. Riès-Kautt, R. Menez, A. Ducruix, Acta Crystallogr. B 48 (1992) 520.
- [20] L. Howel, Acta Cryst. D 51 (1995) 654.
- [21] G. Wagner, W. Braun, T.F. Havel, T. Schaubman, N. Go, K. Wuthrich, J. Mol. Biol. 196 (1987) 611.
- [22] S. Lafont, S. Veesler, J.P. Astier, R. Boistelle, J. Cryst. Growth 173 (1997) 132.
- [23] M. Riès-Kautt, A. Ducruix, A. van Dorsselaer, Acta Cryst. D 50 (1994) 366.

- [24] C. Jolivald, M. Riès-Kautt, P. Chevallier, A. Ducruix, J. Synchrotron Rad. 4 (1997) 28.
- [25] D.G. Davis, A. Bax, J. Am. Chem. Soc. 107 (1985) 2821.
- [26] J. Jeener, B.H. Meier, P. Bachman, R.R. Ernst, J. Chem. Phys. 71 (1979) 4546.
- [27] J.-L. Pons, T.E. Malliavin, M.A. Delsuc, J. Biomol. NMR 8 (4) (1996) 445.
- [28] A. Böckmann, E. Guittet, J. Chim. Phys. 92 (1995) 1923.
- [29] G. Otting, E. Liepinsh, J. Biomol. NMR 5 (1995) 420.
- [30] E. Liepinsh, G. Otting, K.J. Wütrich, J. Biomol. NMR 2 (1992) 447.
- [31] G. Otting, E. Liepinsh, B.T. Farmer, K.J. Wüthrich, J. Biomol. NMR 1 (1991) 209.
- [32] R. Brüschweiler, B. Roux, M. Blackledge, C. Griesinger, M. Karplus, R.J. Ernst, J. Am. Chem. Soc. 114 (1992) 2289.
- [33] R. Brüschweiler, P.E. Wright, Chem. Phys. Lett. 229 (1994) 75.
- [34] J.D. Stoesz, R.W. Lumry, Biochemistry 17 (1978) 3693.
- [35] S. Modi, D.V. Behere, S. Mitra, J. Biol. Chem. 264 (33) (1989) 19677.
- [36] G.B. Crull, H.M. Goff, J. Inorg. Biochem. 15 (1993) 181.
- [37] W.L. Galanter, R.J. Labotka, Biochim. Biophys. Acta 1079 (1991) 146.
- [38] S. Modi, D.V. Behere, S. Mitra, Biochemistry 28 (1989) 4689.
- [39] P. Chakrabarti, J. Mol. Biol. 234 (1993) 463.
- [40] G. Otting, E. Liepinsh, K. Wütrich, Biochemistry 32 (1993) 3571.
- [41] J. Deisenhofer, W. Steigemann, Acta Cryst. B 31 (1975) 238.
- [42] G. Otting, K. Wütrich, J. Am. Chem. Soc. 111 (1989) 1871.
- [43] K.S. Kim, J.A. Fuchs, C.K. Woodward, Biochemistry 32 (1993) 9600.
- [44] S.N. Timasheff, Annu. Rev. Biophys. Biomol. Struct. 22 (1993) 67.
- [45] V. Dötsch, G. Wider, J. Am. Chem. Soc. 117 (1995) 6064.
- [46] V.P. Denisov, B. Halle, J. Mol. Biol. 245 (1995) 682.
- [47] J.G.E.M. Fraaije, J. Lyklema, Biophys. Chem. 39 (1991) 31.